CrystEngComm

Accepted Manuscript

ROYAL SOCIETY OF CHEMISTRY

www.rsc.org/crystengcomm

Journal Name

RSCPublishing

COMMUNICATION

Compositionally controlled band gap and photoluminescence of ZnSSe nanofibers by electrospinning

Cite this: DOI: 10.1039/xoxxoooooox

L. J. Chen,[†] C. R. Lee,[†] Y. J. Chuang,[‡] Z. H. Wu,[‡] and C. Chen[§]

Received ooth January 2012,
Accepted ooth January 2012

DOI: 10.1039/xoxxoooooox

www.rsc.org/

A simple, non-toxic, low-priced, and reproduce manipulation, which meets the model of green chemistry, is introduced for the synthesis of ZnS_xSe_{1-x} nanofibers. ZnS_x Se_{1-x} nanofibers have been prepared in the entire composition range from ZnSe to ZnS by using the low cost wet-chemical method. The effects of polymer (PVB) concentrations, reactant (S/Se) concentrations and reaction conditions (applied voltage, viscosity, work distance) have been investigated. We have demonstrated that the wurtzite ZnS_x Se_{1-x} showing fiber-like morphology can be kinetically stabilized in the presence of electrospinning system.

One-dimensional (1D) semiconductor nanomaterials have received much attention for their unique electronic, optical, physical, chemical properties and potential applications in optoelectronics devices, photonics, energy conversion, catalysis, and biosensors.[1-3] Amid the group II-VI semiconductors (ZnSSe) as a direct band gap material with bulk band gap of 2.70 eV~3.5 eV, is considered as a good candidate for light-emitting devices and other optical-electronic devices.[4,5] Band gaps are one of the most significant factors of semiconductor materials for optoelectronic applications since they resolve the spectral characteristic of absorptions and emission processes. Nanomaterials such as nanofibers open a new sight of band gaps through alloying with nearly assertive compositions. [6-8] ZnSe (bulk band gap 2.7 eV) and ZnS (bulk band gap 3.6 eV) are wide band gap semiconductor materials. These wide band gap semiconductors are also charming hosts for the formation of doped nanomaterials.[9,10] For these reasons, synthesis of high quality ZnSe and ZnS nanomaterials is still an attractive topic.[10-16]

An important region in nanotechnology is the fabrication of composite structures containing different semiconductor nanocrystals. In semiconductor nanomaterials, band gap energy can easily be handled by slight tuning in composition and size. The surface morphology also plays an important function in determining the properties of the system, especially at nanoscale cause of their large surface to volume ratio. A concomitant control of morphology and structure of semiconductor nanomaterials provides chances to tune and research their optical properties. The properties of materials change dramatically with size and composition, comprising thermodynamic stability. Also, structural transformations have been demonstrated to occur in nanoscale materials at lower temperatures.[17]

One of the important Zn-based II-VI semiconductors, ZnS_xSe_{1-x} has been intended to be an suitable material for photoelectronic devices due to its wide direct band gap and large giant photoresistivity. [18-20] Moreover, ZnS_xSe_{1-x} is also a promising material for windows, biomedical labels, output couplers, lenses, and optically controlled switching, due to its low absorptivity at infrared wavelength and exciton binding energy. The research efforts in the field of optical control of ZnS_xSe_{1-x} have been mostly focused on fabricating 1D nanofibers by easily electrospinning process (as shown in Figure S1). In the present study, we report the synthesis of ZnS_xSe_{1-x} in the wurtzite phase at a low temperature in the presence of PVB by an annealing condition. ZnS_xSe_{1-x} nanofibers were prepared by the electrospinning of a mixture of selenium and sulfur precursor into the zinc precursor based on previously reported methods (Please see Supporting Information for experimental details).[3, 21-23]The phase and morphology evolutions of ZnS_xSe_{1-x} in the presence of PVB are systematically studied by scanning electron microscope (SEM), transmission electron microscope (TEM), X-ray diffraction (XRD), X-ray photoelectron spectroscopy (XPS), UV-visible, and diode pumped solid state laser (DPSS).

The influence of the parameters of the solution on the morphology of nanofibers was studied. The diameter of PVB/ ZnS_xSe_{1-x} composite fibers obtained at different work distances and concentrations are shown in Figiure 1a. With increasing concentration ratio, the diameter of PVB/ ZnS_xSe_{1-x} composite fibers decreased and bead-on-string structures appeared. When the concentration ratio was promote increased, the beads on fibers reduced, as shown in Figure 1a (blue line). Contrasted with various

concentrations, the capping medium forms stable complexes with the precursor, which the rapid formation of small nanoparticles as the crystal nuclei and slow crystal growth to form nanofibers from the crystal nuclei according to the inherent crystal structure. In this case, the work distance from the tip of the needle to the collector is enough long for the elongation and solidification of the jet to form fibers, as shown in Figure 1a (black line). However, when the work distance was reduced, the fiber diameter increased. That is, the morphology of the electrospinning structure transformed rapidly and one was the evaporation of solvent in the jet was somewhat suppressed. The lashing instability, which facilitated the diffusion of the jet, was extremely suppressed.[24] The results show that a large work distance is preferred for electrospinning.

Figure 1b shows fiber diameters of PVB/ ZnS_xSe_{1-x} composite fibers for various viscosities and applied voltages (10 kV, 15 kV, 20 kV, and 22 kV). The fiber diameter decreased with increasing viscosity, as expected (Figure 1b, black line). One hundred PVB/ ZnS_xSe_{1-x} composite fibers were selected from ten spots of 60 × 60 μm^2 to measure the distribution of the diameters. This may be due to the greater expanded conformation of PVB/ ZnS_xSe_{1-x} in the solution caused by the electrostatic repulsion between PVB/ ZnS_xSe_{1-x} mixture molecules. The molecular entanglement of PVB/ ZnS_xSe_{1-x} in solution is thus expected to be higher. It was observed that the diameter distribution of the PVB/ ZnS_xSe_{1-x} composite fibers decreased with increasing applied voltage (Figure 1b, blue line). The jet is driven by a high electrical potential applied between the collector and the solution. The electrical forces which stretch the wires are resisted by the elongation viscosity of the jet. A reduction in size with the applied voltage has been reported for various electrospinning organic fibers.[25]

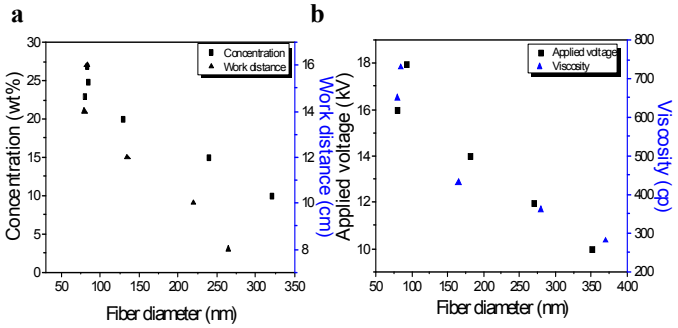

Figure 1. (a) Diameters of PVB/ $ZnS_{0.5}Se_{0.5}$ composite fibers for various concentration ratios and work distances. (b) Diameters of PVB/ $ZnS_{0.5}Se_{0.5}$ composite fibers for various viscosities and applied voltages.

Figure 2 shows a series of SEM images of PVB/ ZnS_xSe_{1-x} nanofibers obtained from precursor solutions with concentration ratios of 5 wt.%, 10 wt.%, 20 wt.%, 23 wt.%, and 27 wt.% (PVB/ethanol content ratio). As can be seen in Figure 2a, lesser fibers were obtained when the ratio was 10 wt.%. Because of the ratio decreased, the conductivity of fibers increased, the viscosity of fibers decreased, and bead-on-string structures appeared. When the ratio further increased, the beads on fibers decreased. The results presented that high concentration preferred generated fibers ratios increased. The high conductivity solvent is helpful to the ion diffusion and reduces resistance. The high viscosity solvent can generate the diffusion of ions not to be easy, to reduce the conductivity.[26] When the concentration of PVB was increased, bead-on-string structures were noted, as shown in Figure 2b-d, and the bead density decreased. PVB/ ZnS_xSe_{1-x} nanofibers with smooth surfaces were obtained when the PVB/ethanol ratio was 23 wt.%. The concentration of PVB is accordingly a key factor in the preparation of smooth PVB/ ZnS_xSe_{1-x} nanofibers. PVB acted as the capping medium, which in the PVB/ ZnS_xSe_{1-x} composite nanofibers exist states is adsorbed polymer chains induce not only steric repulsion but also bridging attraction. Pure PVB fibers are shown in Figure 2e; their morphology is smooth than those of PVB/ ZnS_xSe_{1-x} fibers. Figure S2 shows TGA thermogram of the PVB/ ZnS_xSe_{1-x} nanofibers. It was observed that the weight essentially decreases in the low temperature region. The higher thermal stability of PVB/ ZnS_xSe_{1-x} fiber might be attributed to its higher chain compactness due to the interaction between the PVB and the ZnS_xSe_{1-x} materials.[27-29] It is clear from the TG curve that all the PVB and the organic group were removed completely at 680 °C, resulting in a metal oxide composite phase.[30]

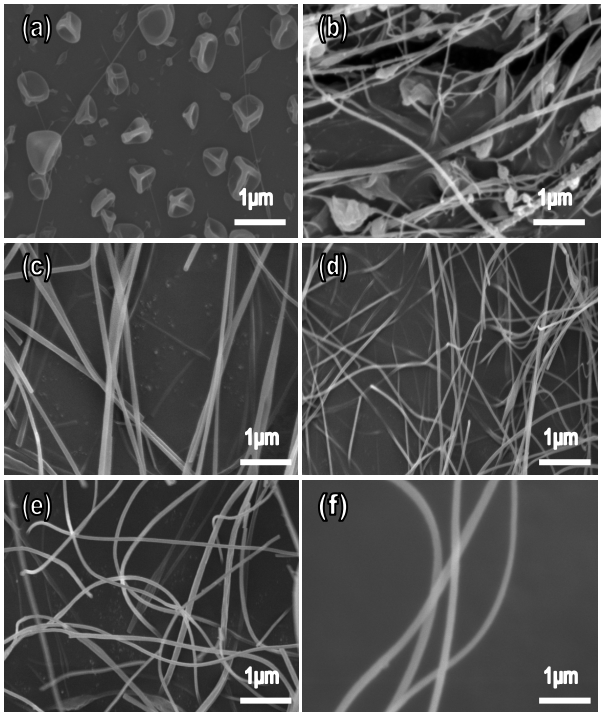

Figure 2. SEM images of PVB/ $ZnS_{0.5}Se_{0.5}$ composite nanofibers electrospinning from (a) 5 wt.%, (b) 10 wt.%, (c) 20 wt.%, (d) 23 wt.%, (e) 27 wt.% aqueous solutions at 16 kV, and (f) pure PVB fibers.

ZnS and ZnSe have been known to crystallize with both cubic (zinc-blende) and wurtzite (hexagonal) structures.[31] For this motive, it is important to prove the crystal structure of the synthesized nanofibers. The phase recognition was carried out by X-ray diffraction (XRD) as shown in Figure 3a. The average crystal domain size of the nanocrystals calculated using Scherrer's equation based on the (100) peak is 75 nm ($D = K\lambda/(\beta\cos\theta)$; K = 0.89, λ= 0.15418 nm, β= FWHM, θ= diffraction angle). The zinc sulfide (zinc selenium) major diffraction peaks observed at 26.9, 28.5, 30.52, 39.61, 47.56, 51.77, 55.5, and 56.39° 2θ (25.86, 27.39, 29.3, 38.03, 45.61, 49.64, 53.18, and 54.03° 2θ) can be indexed to the (100), (002), (101), (102), (110), (103), (200), and (112) of the wurtzite (hexagonal) crystal structure, respectively. Then, in order to determine that the nanocrystals are hexagonal, it is crucial to observe the minor peaks that are unique to the hexagonal structure. For example, the minor peaks at 55.5°, 57.5°, and 63.5° (53.18°, 55.16°,

and 60.85°) corresponding to the (200), (201), and (202) peaks, respectively, are unique to the hexagonal structure (JCPDS 36-1450 and 80-0008) and are shown as Figure 3a. The ZnS_xSe_{1-x} nanocrystal diffraction peaks also show patterns gradually shifting toward a lower angle with decreasing sulfide content, due to the decreased lattice spacing with smaller sulfide atoms substituting for larger selenium atoms (Figure S3). Similar behavior could be found in the literature.[32,33] The morphology of the $ZnS_{0.5}Se_{0.5}$ nanofibers was characterized using a transmission electron microscope (H-800) with an acceleration voltage of 160 kV. Figure 3b shows TEM images of $ZnS_{0.5}Se_{0.5}$ nanofibers by electrospinning at 18 kV. The fiber-like nanostructures have diameters from 70 to 80 nm and lengths from hundreds of nanometers to several micrometers. By changing the reaction concentration, viscosity, collector distance, and applied voltage, the nanofiber size can be easily controlled. When the PVB/ethanol ratio was increased from 10 wt.% to 27 wt.% with a tip-to-collector distance of 14 cm, the diameters decreased to about 75 nm. The growth directions for the nanofibers were determined from the selected area electron diffraction (SAED) patterns shown in the inset in Figure 3c. A high-resolution bright field TEM image of characteristic nanofibers from the wurtzite synthesis is shown in Figure 3b. The image is taken along the $[01\bar{1}0]$ zone axis with the (220), (204), and (024) crystallographic planes indicated by white lines. Spacing measurements based on 6 planes indicated d-spacings of 2.94 ± 0.02 Å for the (220) and 3.12 ±0.02 Å for the (204) and (024). The measured angle between the (220) and (024) planes is 56.5 ± 0.5° and is 62 ± 0.5° between (204) and (024) planes. If the structure were cubic, the measured angles should be 60° between all three planes, and the measured d-spacings should be 3.12 Å. These observed differences provide additional evidence of lattice distortion that result from cation ordering and the wurtzite crystal structure. The zone axis of the SAED pattern was determined to be [0001], and the pattern is typical for nanocrystals from this similar synthesis process. These extra spots correspond to 2/3 the distance of the (114) or (122) fundamental reflections and have a d-spacing of 3.1 Å. Both high-resolution TEM (Figure 3b) and XRD (Figure 3a) confirmed that the nanocrystals are crystalline with hexagonal wurtzite structure. No other crystal phases were observed in the XRD patterns of the product. Compositional analysis by XPS and quantum yield showed that the average composition of the nanocrystals in the sample has a molar Zn/Sn/S ratio of 1:x:1-x (x=0, 0.2, 0.5, 0.8 and 1, respectively.) and the composition of individual particles measured by EDS were 1:x:1-x with a variation from particle to particle less than the experimental error of ca. ±2 atom % (see Table S1 and Figure S4).

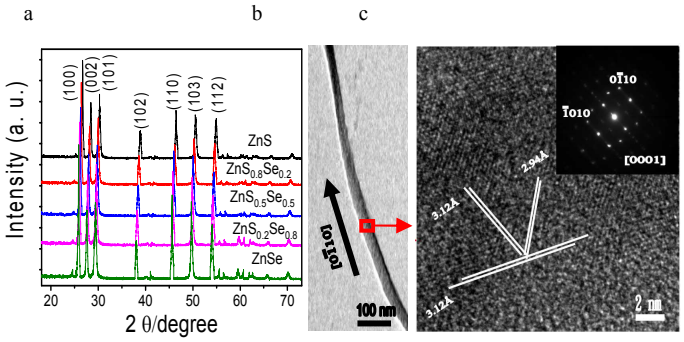

Figure 3. (a). X-ray diffraction patterns of as-synthesized ZuS_xSe_{1-x} nanofibers at different S/Se ratio values as a function of x=0, 0.2, 0.5, 0.8 and 1. (b) TEM images of as-synthesized $ZnS_{0.5}Se_{0.5}$ nanofibers and SAED pattern (inset) and (c) high-resolution TEM of wire-like $ZnS_{0.5}Se_{0.5}$ nanostructures recorded along [0001].

The purity and composition of synthesized ZnSSe were examined by XPS analyses. The typical XPS results are shown in Figure S5, including (a) Zn 2p, (b) S 2p, and (c) Se 3d. In Figure S5a, the Zn core-level spectrum was presented with the binding energies of 1021.6 corresponding to $2p_{1/2}$, which are very similar to the previous report.[3,34] In Figure S5b, the S 2p core-level spectrum was presented with an optimal curve fitting for the distinct peak at the binding energy of 161.2 eV corresponding to $2p_{3/2}$.[3] In Figure S5c, the Se 3d core-level spectrum was presented at the binding energy of 54.81 eV corresponding to $3d_{3/2}$.[35] The steady-state absorption spectra of the ZnS_xSe_{1-x} nanofibers are shown in Figure 4a with the absorption of the nanofibers normalized at 420 nm. A significant red shift is observed for samples with different ratios. The absorption band is continuously shifted to 356.32 nm (3.48 eV) for the ZnS_xSe_{1-x} nanofibers (x=1), to 383.9 nm (3.23 eV) for the ZnS_xSe_{1-x} nanofibers (x=0.8), to 405.22 nm (3.06 eV) for the the ZnS_xSe_{1-x} nanofibers (x=0.5), to 436.62 nm (2.84 eV) for the ZnS_xSe_{1-x} nanofibers (x=0.2), and further to 467.92 nm (2.65 eV) for the ZnS_xSe_{1-x} nanofibers (x=0). The initial absorbance band position gradually shifts to long wavelength after selenium doped. The optical band gap for the ZnS_xSe_{1-x} nanofibers (S:Se = 1:0, 0.8:0.2, 0.5:0.5, 0.2:0.8 and 0:1) can be calculated as a direct transition between model parabolic bands using the Tauc equation. The Tauc equation can be used to estimate the optical band gap in a semiconductors from its UV−vis absorption spectrum:[36]

$$(\alpha h\upsilon)^n = B\left(E - E_g^{Tauc}\right)$$

where α is the absorption coefficient, h is Planck's constant, ν is the frequency of radiation, n = 2 for a direct band gap semiconductor material (such as ZnSSe), B is a constant of proportionality, E is the energy of the electromagnetic radiation (equal to hν), and E_g^{Tauc} is the band gap energy measured by the Tauc plot.The estimated optical band gap for each S:Se ratio was shown in Figure 4b. Similar to the crystal lattice spacing seen with TEM and XRD, the optical band gap can be tuned from 3.48 eV in pure ZnS nanofibers to 2.65 eV in pure ZnSe nanofibers simply by the stoichiometry of the TOPOSeS precursor. In addition to the absorption spectra, the photoluminescence spectra of the ZnS, $ZnS_{0.8}Se_{0.2}$, $ZnS_{0.5}Se_{0.5}$, $ZnS_{0.2}Se_{0.8}$, and ZnSe are shown in Figure 4c. Emission spectra were recorded using a pumped-pulse laser beam from a Q-switch Nd:YAG laser (LAB-130, from Quanta-Ray,) with 442 nm and 532 nm excitation. The red shifts of emission peak from 493 nm for pure ZnS nanofibers to 621 nm for pure ZnSe nanofibers.

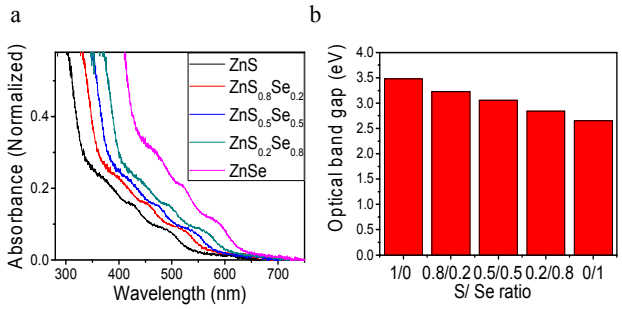

c

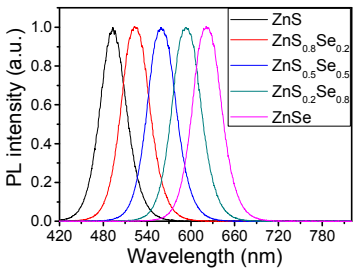

Figure 4. (a) UV-vis absorption spectra of ZnS_xSe_{1-x} nanofibers synthesized at various ratio values as a function of x=1, 0.8, 0.5, 0.2 and 0. (b) Variation of band gap with composition ZnS_xSe_{1-x} nanofibers. (c) PL spectra of the ZnS_xSe_{1-x} nanofibers with various S/Se ratio dispersed in toluene. The S ratio decrease from left to right through 1, 0.8, 0.5, 0.2 and 0, respectively. The excitation wavelength is 442 nm (x=1 and 0.8) and 532nm (x=0.5, 0.2 and 0).

Conclusions

A low cost electrospinning synthetic approach of designing ZnS_xSe_{1-x} nanofibers offers a simple methodology for tuning the optical properties across the entire compositional range from pure ZnS to pure ZnSe. By varying the S:Se precursor ratio we were able to tune the optical band gap of the ZnS_xSe_{1-x} nanobers from 2.65 to 3.48 eV. These ZnS_xSe_{1-x} nanofibers were found to be highly crystalline, Wurtzite phase, and grew along the $[01\bar{1}0]$ direction. A strong visible PL emission is estimated for ZnS_xSe_{1-x} showed an all optical emission band from 490 to 630 nm. ZnS_xSe_{1-x} nanofibers with great potential applications in optoelectronics, photonic devices, photocatalysis, biosensor, drug targeting, diagnostic analysis and white illumination source.

Acknowledgements

The authors would like to thank the Ministry of Science and Technology, Taiwan (MOST) (contract 103-2112-M-006-016-MY3) and Department of Photonics, National Cheng Kung University for supporting this research.

Notes and references

†Department of Photonics, National Cheng Kung University, Tainan, Taiwan
E-mail: linjerchen@hotmail.com, linjer@mail.ncku.edu.tw

‡Department of Materials Science and Engineering, National Cheng Kung University, Tainan, Taiwan

§Department of Chemistry, National Cheng Kung University, Tainan, Taiwan.

Electronic Supplementary Information (ESI) available: Synthesis and characterization details, thermogravimetric analysis (TGA) curves, X-ray diffraction (XRD) pattern and typical XPS spectra of the synthesized wurtzite ZnS_xSe_{1-x} nanofibers. See DOI: 10.1039/c000000x/

1 H. Li , X. Wang , J. Xu , Q. Zhang , Y. Bando , D. Golberg , Y. Ma and T. Zhai, *Adv. Mater.,* 2013, **25**, 3017.

2 F. Shiba, T. Tamagawa, T. Kojima and Y. Okawa, *CrystEngComm,* 2013, *15*, 1061.

3 R. Jing, A. Shan, R. Wang and C. Chen, *CrystEngComm*, 2013, 15, 3587.

4 X. T. Zhang, K. M. Ip, Z. Liu, Y. P. Leung, Q. Li and S. K. Hark, *Appl. Phys. Lett.,* 2004, **84**, 2641.

5 S. Jana, B. B. Srivastava, S. Acharya, P. K. Santra, N. R. Jana, D. D. Sarmac and N. Pradhan, *Chem. Commun*., 2010, **46**, 2853–2855.

6 P. Narang, S. Chen, N. C. Coronel, S. Gul, J. Yano, L. W. Wang , N. S. Lewis and H. A. Atwater, *Adv. Mater.,* 2014, **26**, 1235.

7 A. Pan, R. Liu, M. Sun and C. Ning, *J. Am. Chem. Soc.,* 2009, **131**, 9502.

8 L. J. Chen, J. D. Liao, Y. J. Chuang, Y. S. Fu, *J. Am. Chem. Soc.,* 2011, **133**, 3704.

9 T. Trindade, P. O'Brien and N. L. Pickett, *Chem. Mater.,* 2001, **13**, 3843.

10 V. Lesnyak, A. Dubavik, A. Plotnikov, N. Gaponik and A. Eychmu¨ller, *Chem. Commun.*, 2010, **46**, 886–888.

11 A. Shavel, N. Gaponik and A. Eychmller, *J. Phys. Chem. B* 2004, **108**, 5905.

12 Y. Zhang, H. Xu and Q. Wang, *Chem. Commun*., 2010, **46**, 8941–8943.

13 X. Wu, P. Jiang, Y. Ding, W. Cai, S. S. Xie, and Z. L. Wang, *Adv. Mater.* 2007, **19**, 2319–2323.

14 W. Jia, B. Jia, X. Wu and F. Qu, *CrystEngComm*, 2012, **14**, 7759–7763.

15 W. Jia, B. Jia, F. Qu and X. Wu, *Dalton Trans,* 2013, **42**, 14178-87.

16 L. Hu , J. Yan , M. Liao , H. Xiang , X. Gong , L. Zhang and X. Fang, *Adv. Mater.* **2012**, *24*, 2305–2309.

17 C. S. Tiwary, C. Srivastava and P. J. Kumbhakar, *Appl. Phys.,* 2011, **110**, 034908.

18 L. H. Zhang, H. Q. Yang, J. Yu, F. H. Shao, L. Li, F. H. Zhang and H. J. Zhao, *Phys. Chem. C,* 2009, **113**, 5434.

19 L. W. Yin and S. T. Lee, *Nano Lett.,* 2009, **9**, 957.

20 M. Wang, G. T. Fei, Y. G. Zhang, M. G. Kong and L. D. Zhang, *Adv. Mater.,* 2007, **19**, 4491.

21 Y. J. Chuang, J. D. Liao and L. J. Chen, *J. Compos Mater.*, 2012, **46**, 227.

22 L. J. Chen, J. D. Liao, Y. J. Chuang and Y. S. Fu, *Polymer,* 2011, **52**, 116.

23 J. M. Deitzel, J. Kleinmeyer, D. Harris and N. C. Beck Tan, *Polymer,* 2001, **42**, 261.

24 D. H. Reneker and I. Chun, *Nanotechnology*, 1996, **7**, 216.

25 S. G. Lee, S. S. Choi and C. W. Joo. *J Korean Fiber Soc,* 2002, **39**, 1.

26 P. Ruenraroengsak and A. T. Florence, *Int J Pharm,* 2005, **298**, 361.

27 M. R. Karim, H. W. Lee, R. Kim, B. C. Ji, J. W. Cho and T. W. Son, *Carbohydr Polym,* 2009, **78**, 336e42.

28 Y. Y. Chen and W. C. J. Wei, *J Eur Ceram Soc,* 2001, **21**, 2535e40.

29 W. Liu, D. B. Mitzi, M. Yuan, A. J. Kellock, S. Jay Chey and O. Gunawan, *Chem Mater,* 2010, **22**, 3.

30 S. M. Kim, G. S. Kim and S.Y. Lee, *Mater. Lett.* 2008, *62*, 4354.

31 J. Baars and G. Brandt, *J. Phys. Chem. Solids,* 1973, **34**, 905.

32 M. G. Panthani, V. Akhavan, B. Goodfellow, J. P. Schmidtke, L. Dunn, A. Dodabalapur, P. F. Barbara and B. A. Korgel, *J. Am. Chem. Soc.,* 2008, **130**, 16770.

33 D. Pan, X. Wang, Z. H. Zhou, W. Chen, C. Xu and Y. Lu, *Chem. Mater.,* 2009, **21**, 2489.

34 S. Shen, Y. Zhang, Y. Liu, L. Peng, X. Chen and Q. Wang, *Chem. Mater.,* 2012, **24**, 2407.

35 S. Li, Z. Zhao, Q. Liu, L. Huang, G. Wang, D. Pan, H. Zhang and X. He, *Inorg. Chem.,* 2011, **50**, 11958.

36 S. Mehta, S. Kumar, S. Chaudhary, K. Bhasin and M. Gradzielski, *Nanoscale Res. Lett.,* 2009, **4**, 17.

Graphical abstract